Journal of Hazardous Materials 178 (2010) 349–355

Contents lists available at ScienceDirect

Journal of Hazardous Materials

journal homepage: www.elsevier.com/locate/jhazmat

Application of AlMCM-41 for competitive adsorption of methylene blue and rhodamine B: Thermodynamic and kinetic studies

S. Eftekhari, A. Habibi-Yangjeh*, Sh. Sohrabnezhad

Department of Chemistry, University of Mohaghegh Ardabili, P.O. Box 179, Ardabil, Iran

ARTICLE INFO

Article history:
Received 8 July 2009
Received in revised form
30 December 2009
Accepted 18 January 2010
Available online 25 January 2010

Keywords:
Competitive adsorption
AlMCM-41
Adsorption kinetic
Adsorption isotherm
Methylene blue
Rhodamine B

ABSTRACT

AlMCM-41 was applied for adsorption of methylene blue (MB) and rhodamine B (RB) in single and binary component systems. In the single component systems, AlMCM-41 represents higher adsorption capacity for MB than RB with the maximal adsorption capacity of 2.08×10^{-4} and 8.74×10^{-5} mol/g at 25 °C for MB and RB, respectively. In the binary component system, MB and RB exhibit competitive adsorption onto the adsorbent. The adsorption is approximately reduced to 94 and 79% of single component adsorption systems for MB and RB (initial concentration of 8×10^{-6} M) at 25 °C. In single and binary component systems, kinetic and adsorption isotherm studies demonstrate that the data are following pseudo-second-order kinetic model and Langmuir isotherm. Effect of solution pH on the adsorption in single and binary component systems was studied and the results were described by electrostatic interactions.

1. Introduction

Many industries use dyes to color their products and also consume substantial volumes of water. The presence of small amounts of dyes in water is highly visible and undesirable [1]. The removal of dyes from wastewaters is of a great concern nowadays, because many dyes and their degradation products are toxic and carcinogenic, posing a serious hazard to aquatic living organisms [2]. Various treatment processes such as physical separation, chemical oxidation and biological degradation have been widely investigated to remove dyes from wastewaters [3,4]. Adsorption techniques have proved to be an effective and attractive process for removal of non-biodegradable pollutants (including dyes) from wastewaters [5–7].

Recently, mesoporous compounds produced by the Mobil Oil Corporation, called MCM (Mobil Composition of Matter), show very interesting properties [8]. Due to the high surface area and nanometer sized pore of the mesoporous compounds, especially MCM-41 been believed the promising materials as adsorbents for various inorganic ions and organic dyes [9–20]. Incorporation of aluminum into the structure of MCM-41 materials *via* isomorphous substitution of aluminum for silicon, generate ion exchange sites in this mesoporous molecular sieve [21,22]. Therefore, cationic dyes such as methylene blue (MB) and rhodamine B (RB) can be adsorbed into AlMCM-41. The calcined AlMCM-41 has a specific surface area of 940 m^2/g and pore size of 24.4 Å [23]. These values are similar to the corresponding values for MCM-41 (surface area = 1027 m^2/g and pore size = 25.3 Å). Therefore, incorporation of aluminum does not alter considerably surface area and pore size of the AlMCM-41. Then, AlMCM-41 has potential for liquid-phase adsorptions. Recently, it has been indicated that adsorption of cationic dyes on AlMCM-41 taken place *via* ion exchange method [23]. Moreover, AlMCM-41 was applied by Sohrabnezhad (one of authors) as support for photocatalytic degradation of MB [24].

In the last few years, various adsorbents have been applied for adsorption of organic dyes from aqueous solutions. In these studies, mainly, single component systems have been investigated [25–30]. As most industrial wastewaters contain more than one pollutant, an investigation into the effects of multisolute systems on adsorption capacity is practically important. Thus, in the present study, for a first time, we report single and binary component adsorption kinetic and thermodynamic for adsorption of MB and RB on AlMCM-41.

2. Materials and methods

2.1. Dyes

The dyes are MB and RB and were obtained from Merck. Chemical structures of the dyes are presented in Fig. 1. For preparation of

* Corresponding author. Tel.: +98 451 5512201; fax: +98 451 5512200.
E-mail address: ahabibi@uma.ac.irE (A. Habibi-Yangjeh).

0304-3894/$ – see front matter © 2010 Elsevier B.V. All rights reserved.
doi:10.1016/j.jhazmat.2010.01.086

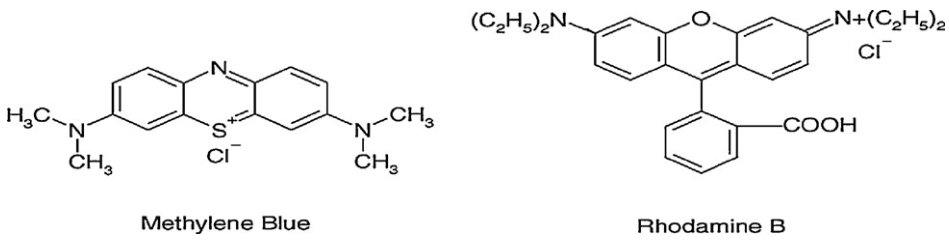

Fig. 1. Chemical structures for methylene blue (MB) and rhodamine B (RB).

solutions, stock solutions with concentration of 10^{-3} M were prepared and the solutions for adsorption tests were prepared from the stock solutions to the desired concentration (10^{-6} to 10^{-5} M). The pH of solutions was adjusted with HCl or NaOH (from Merck) solutions.

2.2. Preparation of AlMCM-41

The MCM-41 and AlMCM-41 materials were synthesized by a room temperature method with some modifications in the described procedure in literature [31]. We used tetraethylorthosilicate (TEOS from Merck) as a source of silicon and hexadecyltrimethylammonium bromide (CTABr from BOH) as a surfactant template for preparation of the mesoporous material. The molar composition of the reactants is as follows:

SiO_2: 1.6EA : 0.215CTABr : 325H_2O

where EA stand for ethylamine. The prepared MCM-41 was calcined at 550 °C for 5 h to decompose the surfactant and obtain the white powder. This powder was used as the parent material to prepare AlMCM-41 by ion-exchange method with 0.1 M solution of $Al_2(SO_4)_3{\cdot}18H_2O$ (from Merck).

2.3. Adsorption test

Adsorption kinetics and isotherm experiments for the samples were undertaken in a batch reactor with 250 ml capacity provided with water circulation arrangement to maintain the temperature at desired value. Adsorption of the dyes was performed by shaking 0.005 g of AlMCM-41 in 200 ml of solutions with varying concentrations (10^{-6} to 10^{-5} M) at 25 and 40 °C. The samples were collected by separation of AlMCM-41 from solution using a centrifuge. UV–vis absorption spectra were recorded by a Shimadzu 1600 PC. Concentration of dyes was determined spectrophotometrically by measuring absorbance at 668 and 556 nm for λ_{max} of MB and RB, respectively (Fig. 2). The data obtained from the adsorption tests were used to calculate the adsorption capacity, q_t (mol/g), of the adsorbent by a mass–balance relationship, which represents the amount of adsorbed dye per amount of the dry adsorbent:

$$q_t = \frac{(C_0 - C_t)V}{W} \quad (1)$$

where C_0 and C_t are concentrations of the dyes in solution (mol/dm^3) at time $t = 0$ and $t = t$, respectively. V is the volume of the solution (dm^3) and W is weight of the dry adsorbent (g).

3. Results and discussion

3.1. Adsorption in single component systems

Fig. 3 demonstrates the dynamic adsorption of MB and RB onto AlMCM-41 at 25 and 40 °C. As can be seen, adsorption of MB and RB on the adsorbent reaches equilibrium approximately at 300 min. This time is very shorter than corresponding time for natural zeolites [28,32]. Also, one can see that adsorption of MB and RB is fast at initial times and then approaches equilibrium at longer times. The time profile for adsorption of the dyes is single, smooth and continuous curve leading to saturation, suggesting the possible monolayer coverage of the dyes on surface of the adsorbent. Also, AlMCM-41 exhibits higher adsorption for MB than RB due to its smaller molecular size than RB, which can be seen in Fig. 1. For the same adsorbent, molecules with larger size will not easily penetrated into the inner pores of the adsorbent, resulting in lower adsorption capacity [26]. Similar results have been reported for adsorption of MB and RB on various adsorbents [26,28]. The adsorption capacity for MB and RB in initial concentration of 1×10^{-5} M at 25 °C is 2.08×10^{-4} and 8.74×10^{-5} mol/g, respectively. The corresponding values for adsorption of MB and RB onto natural zeolite are 5.5×10^{-5} and 2.0×10^{-5} mol/g [28]. Then, it can be concluded that adsorption capacity of AlMCM-41 toward MB and RB adsorption is very greater than natural zeolite. Also, adsorption capacity of MB on MCM-41 is 3.7×10^{-5} mol/g which is very lower than the corresponding value for adsorption onto AlMCM-41 (2.08×10^{-4} mol/g). This can be attributed to the electrostatic interaction between AlMCM-41 with negative charge and MB with positive charge [23].

As can be seen from Fig. 3, temperature influences the adsorption capacity. For the dyes, the adsorption at 25 °C is greater than that of 40 °C, suggesting the exothermic characteristic of the adsorption.

3.1.1. Adsorption isotherm in single component systems

An adsorption isotherm demonstrates that how the adsorbate molecules partition between the liquid and solid phases when the adsorption process reaches equilibrium. The adsorption isotherm is fundamental in describing the interactive behavior between solutes and adsorbent and is important in the design of adsorption systems [28]. Several adsorption isotherms are available. Adsorption of organic dyes on various adsorbents usually obeys Langmuir isotherm [28,30,33]. The Langmuir adsorption is based on assumption of monolayer adsorption on a structurally homogeneous adsorbent, where all the sorption sites are identical and energetically equivalent. Where in, the adsorption occurs at specific homogeneous sites within the adsorbent and once a dye molecule occupies a site, no further adsorption can take place at that site. The equation is as follows:

$$q_e = \frac{K_L q_{max} C_e}{1 + K_L C_e} \quad (2)$$

where q_e is the equilibrium dye concentration on adsorbent (mol/g), C_e is the equilibrium concentration of the dye in solution (mol/l), q_{max} is the monolayer adsorption capacity of adsorbent (mol/g). The Langmuir constant (K_L) is a measure of the affinity between adsorbate and adsorbent and related to the free energy of adsorption [26]. A linear expression for the Langmuir equation is:

$$\frac{C_e}{q_e} = \frac{1}{q_{max} K_L} + \frac{C_e}{q_{max}} \quad (3)$$

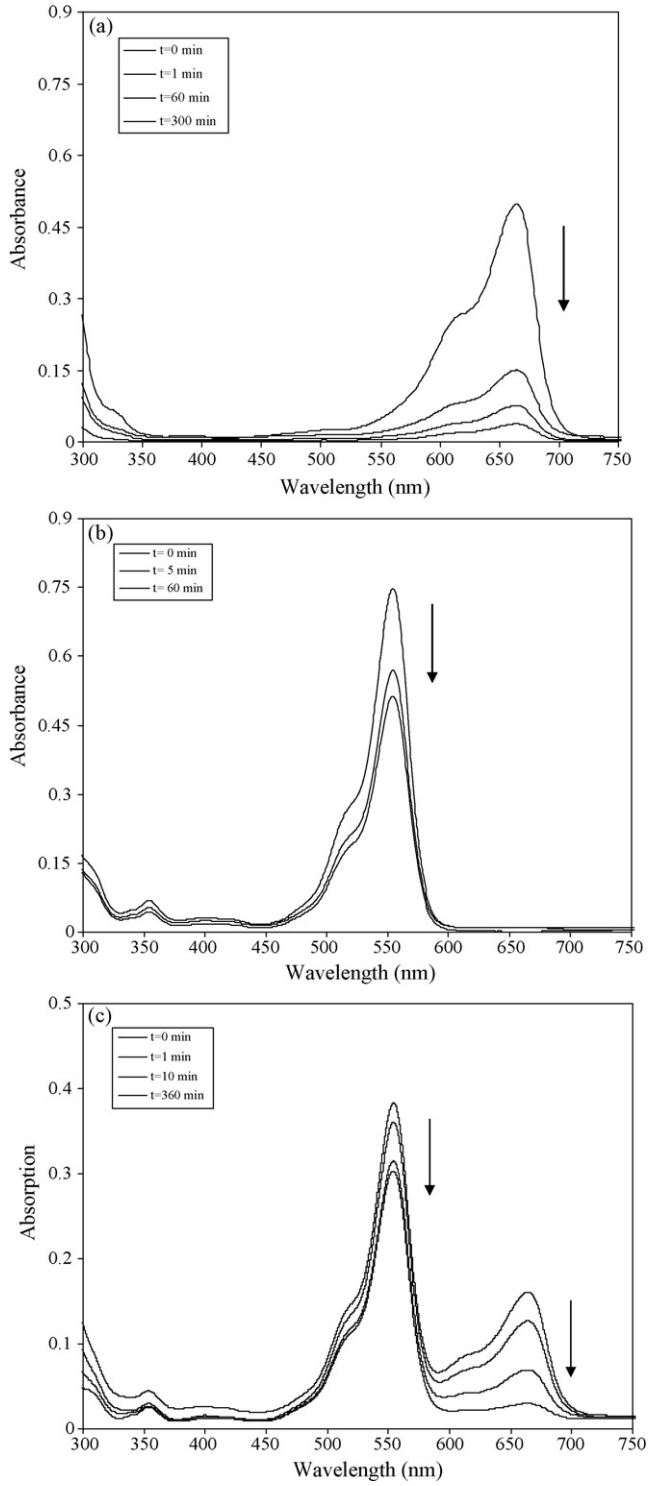

Fig. 2. UV–vis absorption spectra for aqueous solutions of (a) MB, (b) RB and (c) both of the dyes along with AlMCM-41 in various adsorption times at 25 °C.

Plots of C_e/q_e *versus* C_e give a straight line of slope $1/q_{max}$ and intercept $1/q_{max}K_L$.

Fig. 4 shows the linearized Langmuir model for adsorption of MB and RB onto AlMCM-41 at 40 °C. The parameters obtained from the experimental data using the isotherm and the related correlation coefficients are presented in Table 1. One can see that regression coefficients are closer to unity. Then, it can be concluded that the adsorption of both dyes obeys fairly from Langmuir isotherm. Based on the Langmuir isotherm, the maximum adsorption of

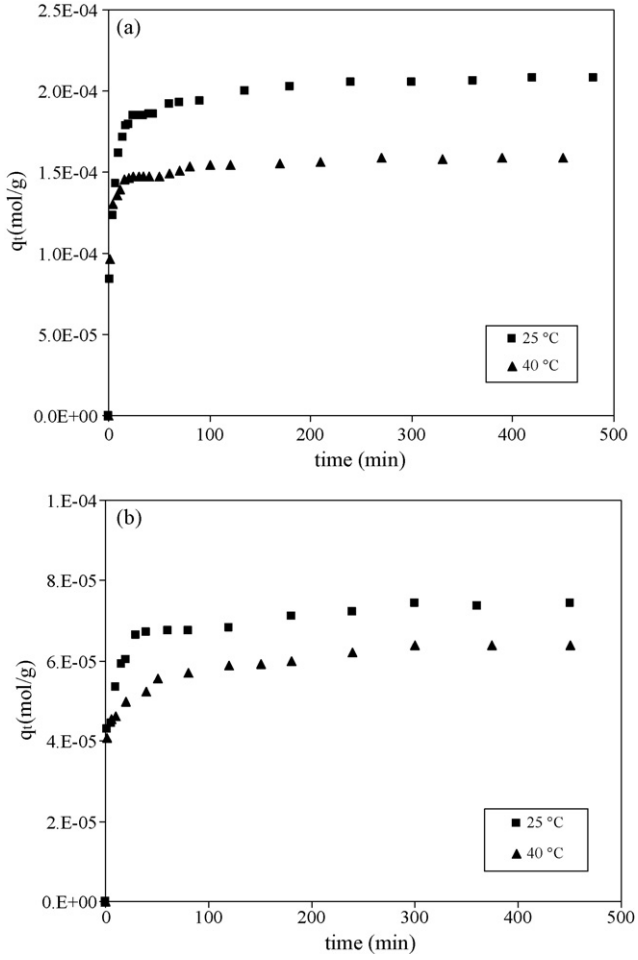

Fig. 3. Dynamic adsorption of MB and RB onto AlMCM-41 at 25 and 40 °C for (a) MB and (b) RB in initial concentration of 8.0×10^{-6}.

MB and RB are 2.08×10^{-4} and 1.19×10^{-4} mol/g, respectively at 25 °C.

Based on the adsorption constant in the Langmuir isotherm (K_L), thermodynamic parameters (ΔG°, ΔH° and ΔS°) for adsorption of MB and RB onto AlMCM-41 were calculated using Eqs. (4)–(6) and the results were tabulated in Table 2. In Eq. (5), K_{L1} and K_{L2} are adsorption constant at T_1 and T_2.

$$\Delta G^\circ = -RT \ \ln K_L \quad (4)$$

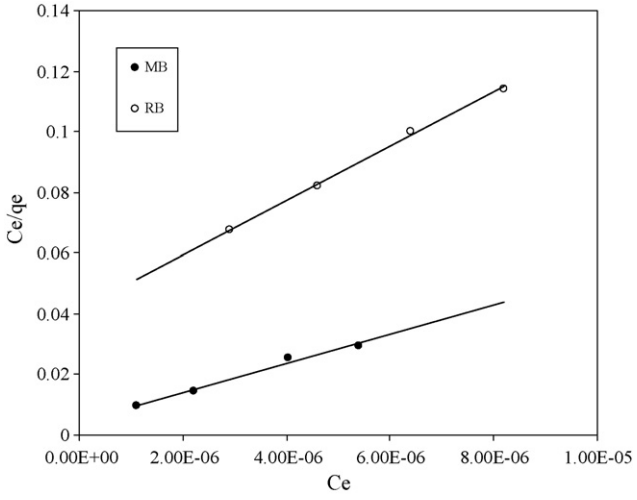

Fig. 4. Langmuir plots for adsorption of MB and RB onto AlMCM-41 at 40 °C.

Table 1
Isotherm parameters for adsorption of MB and RB onto AlMCM-41 in single and binary component systems.

Dyes	Temperature (°C)	Single component			Binary component		
		q_{max} (mol/g)	K_L (1/mol)	R^2	q_{max} (mol/g)	K_L (1/mol)	R^2
RB	25	1.19×10^{-4}	3.07×10^{5}	0.9724	6.07×10^{-5}	4.11×10^{6}	0.9997
	40	1.11×10^{-4}	2.18×10^{5}	0.9979	4.56×10^{-5}	2.65×10^{5}	0.9957
MB	25	2.08×10^{-4}	9.58×10^{6}	0.9982	2.06×10^{-4}	4.83×10^{6}	0.9986
	40	2.08×10^{-4}	1.06×10^{6}	0.9854	1.83×10^{-4}	1.36×10^{6}	0.9959

Table 2
Thermodynamic parameters for adsorption of MB and RB onto AlMCM-41 in single component systems.

Dyes	Temperature (°C)	ΔG° (kJ/mol)	ΔH° (kJ/mol)	ΔS° (J/mol K)
RB	25	−31.30	−17.92	44.89
	40	−31.97		
MB	25	−39.82	−102.0	−208.8
	40	−36.10		

$$\Delta H^\circ = -R\left(\frac{T_2 T_1}{T_2 - T_1}\right)\ln\frac{K_{L1}}{K_{L2}} \quad (5)$$

$$\Delta S^\circ = \frac{\Delta H^\circ - \Delta G^\circ}{T} \quad (6)$$

As can be seen, the adsorption process is spontaneous with the negative value of ΔG°. The standard enthalpy change (ΔH°) for the adsorption of the dyes on AlMCM-41 is negative, indicating that the process is exothermic in nature with ΔH° of −17.92 and −102.0 kJ/mol for RB and MB, respectively.

3.1.2. Adsorption kinetics in single component systems

The kinetic study of adsorption processes provides useful data regarding the efficiency of adsorption and feasibility of scale-up operations. To evaluate the effectiveness of an adsorbate, studies on kinetics of adsorption are also needed [32].

The kinetics of adsorption can be described using several models. A simple kinetic model is the pseudo-first-order equation [30]:

$$\frac{dq_t}{dt} = k_1(q_e - q_t) \quad (7)$$

where k_1 is rate constant for pseudo-first-order adsorption. After definite integration by applying the initial conditions $q_t = 0$ at $t = 0$ and $q_t = q_t$ at $t = t$, Eq. (7) becomes:

$$\ln(q_e - q_t) = \ln(q_e) - k_1 t \quad (8)$$

The above linear equation can usually be used to estimate q_e from intercept and k_1 from the slope. A pseudo-second-order equation can be expressed as follows:

$$\frac{dq_t}{dt} = k_2(q_e - q_t)^2 \quad (9)$$

where k_2 is rate constant for pseudo-second-order adsorption. After definite integration by applying the initial conditions, we have a linear form as:

$$\frac{t}{q_t} = \frac{1}{k_2 q_e^2} + \frac{1}{q_e}t \quad (10)$$

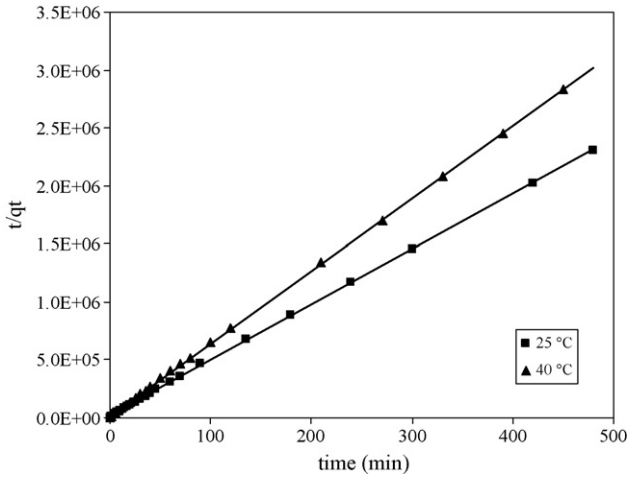

Fig. 5. Pseudo-second-order kinetics for adsorption of MB onto AlMCM-41 at 25 and 40 °C.

The plot of t/qt *versus* time gives straight lines. The values for q_e and k_2 can be calculated from the slope and intercept. Fig. 5 represents plot of pseudo-second-order kinetic model for adsorption of MB at 25 and 40 °C. The kinetic parameters obtained from the models for adsorption of the dyes are given in Table 3. For pseudo-second-order kinetics, the correlation coefficients are closer to unity. This suggests that the adsorption of MB and RB onto AlMCM-41 can be represented better by the pseudo-second-order model.

3.1.3. Effect of solution pH on single component systems

It is known that adsorption of dyes onto adsorbents is influenced by pH of solution [30]. Fig. 6 demonstrates the dynamic adsorption of MB and RB onto AlMCM-41 at three different pH and 25 °C. As can be seen, amount of MB adsorption initially increases as the pH increases and then decreases. When pH of solution is changed from 2 to 7, the adsorption increases from 6.71×10^{-5} to 2.08×10^{-4} mol/g. In acidic solutions, presence of excess H^+ competing with the cationic dyes for adsorption sites. For this reason, the amount of MB and RB adsorption decreases in acidic solutions. It is clear that the amount of RB adsorption greatly decreases as the pH is increasing. When pH of solution is changed from 7 to 12,

Table 3
Kinetic parameters for adsorption of MB and RB onto AlMCM-41 in single component system.

Dyes	Temperature (°C)	Experimental	First-order kinetics			Seconds-order kinetics		
		q_e (mol/g)	q_e (mol/g)	k_1 (h^{-1})	R^2	q_e (mol/g)	k_2 (g/mol h)	R^2
RB	25	8.74×10^{-5}	$5.79 \times 10{-}5$	0.2138	0.8514	8.88×10^{-5}	2.43×10^{6}	0.9995
	40	7.17×10^{-5}	$2.57 \times 10{-}5$	0.0084	0.9306	7.27×10^{-5}	8.85×10^{4}	0.9986
MB	25	2.08×10^{-4}	2.64×10^{-5}	0.0055	0.6778	2.07×10^{-4}	9.29×10^{4}	0.9999
	40	1.84×10^{-4}	3.95×10^{-5}	0.0120	0.7854	1.84×10^{-4}	8.07×10^{4}	0.9998

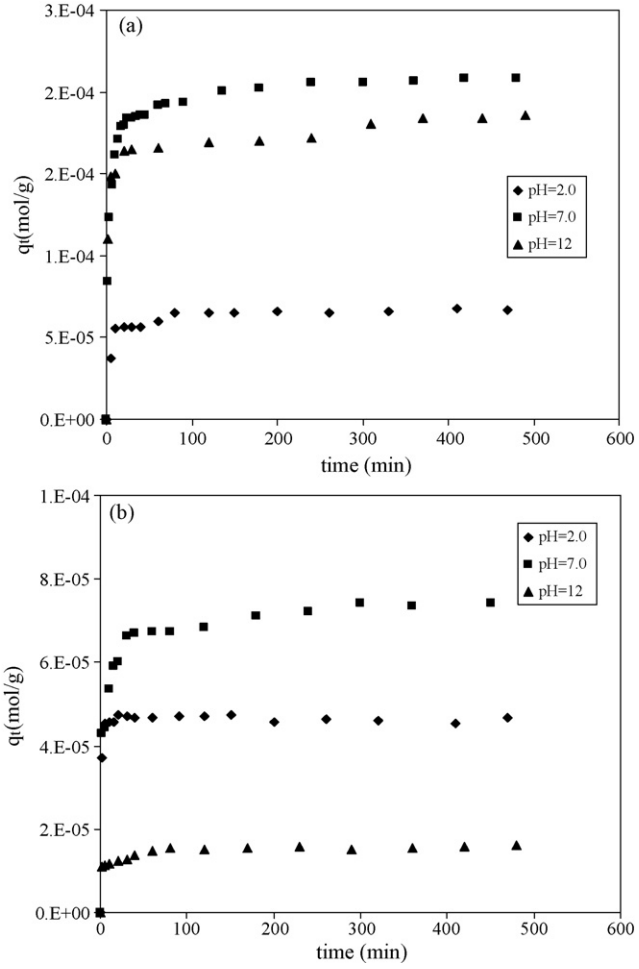

Fig. 6. Dynamic adsorption for MB and RB onto AlMCM-41 in various pH at 25 °C for (a) MB and (b) RB.

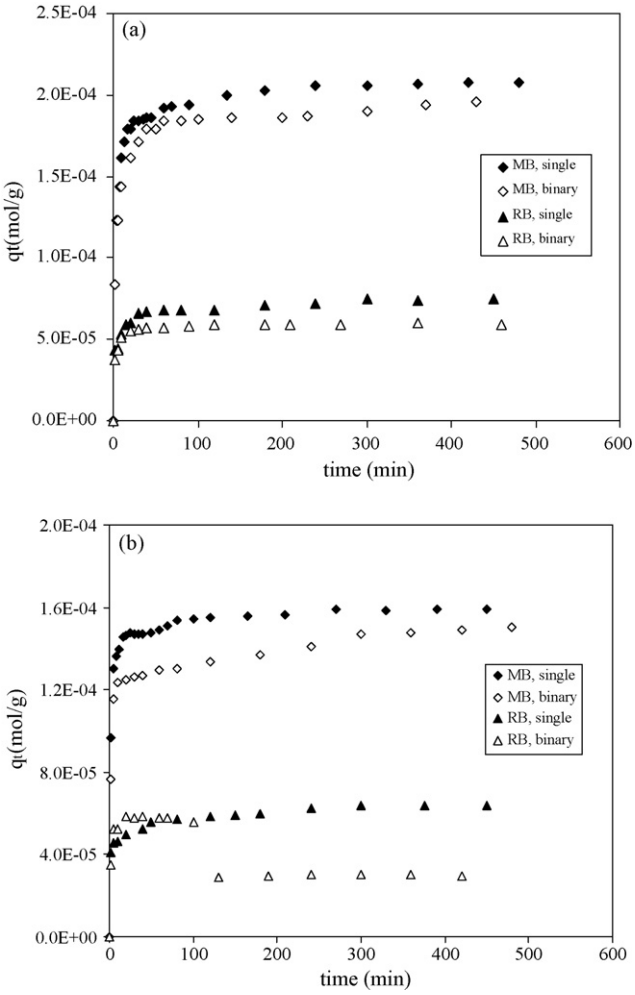

Fig. 7. Comparison of MB and RB adsorption in single and binary component systems at (a) 25 °C and (b) 40 °C.

the adsorption will decrease from 7.43×10^{-5} to 1.62×10^{-5} mol/g. There is a carboxylic group in structure of RB which can be dissociated with increasing pH of solution. Then, in higher pH, RB has zwitterionic character. For this reason, there are not enough electrostatic interactions between negatively charged adsorbent and zwitterionic RB. As a result, amount of the adsorption greatly decreases with pH of solution.

3.2. Adsorption in binary component system

3.2.1. Adsorption isotherm in binary component system

Fig. 7 demonstrates a comparison of MB and RB adsorption onto AlMCM-41 in single and binary component systems at 25 and 40 °C for initial concentration of 8×10^{-6} M. It is clear that the adsorption is reduced in binary component system, which suggests a competitive adsorption. During the process, adsorption reaches an equilibrium adsorption of 1.96×10^{-4} and 5.87×10^{-5} mol/g at initial concentration of 8×10^{-6} M for MB and RB at 25 °C. In binary component system at 25 °C, adsorption of MB and RB is approximately reduced by 94 and 79% of single component adsorption systems, respectively.

The parameters obtained from the experimental data using the linearized Langmuir isotherm for adsorption of MB and RB onto the adsorbent at 25 and 40 °C in binary component system are presented in Table 4. It is clear that similar to single component systems, the competitive adsorption data are fairly fitting in the Langmuir model. By comparing the results in Tables 1 and 4, one can see that the Langmuir constant (K_L) for adsorption of MB and RB in binary component system is lower than single component systems.

In binary adsorption system at 40 °C, it is clear from Fig. 7b that RB adsorption becomes lower after 100 min. Similar results for adsorption on MCM-41 and MCM-48 has been reported [12]. These results were described by reversible adsorption on these adsorbents. Fig. 1 demonstrates that size of RB is larger than MB. Because of smaller size, MB molecules in adsorption process mainly closely packed inside pores of AlMCM-41. For this reason, in single component adsorption system, adsorption capacity of AlMCM-41 toward MB is about 2.4 times greater than RB at 25 °C. However, in binary adsorption system, RB with larger size mainly will adsorb at surface of the adsorbent leading to lower adsorption capacity. Surface adsorbed RB molecules are exposed to hydrolysis in aqueous solutions and thus the attack by water molecules can result releasing of RB from the surface of AlMCM-41 [12]. However, the releasing

Table 4
Thermodynamic parameters for adsorption of MB and RB onto AlMCM-41 in binary component system.

Dyes	Temperature (°C)	ΔG° (kJ/mol)	ΔH° (kJ/mol)	ΔS° (J/mol K)
RB	25	−37.73	−141.8	−349.2
	40	−32.49		
MB	25	−38.13	−65.52	−91.91
	40	−36.75		

Table 5
Kinetic parameters for adsorption of MB and RB onto AlMCM-41 in binary component system.

Dyes	Temperature (°C)	Experimental	First-order kinetics			Second-order kinetics		
		q_e (mol/g)	q_e (mol/g)	k_1 (1/h)	R^2	q_e (mol/g)	k_2 (g/mol h)	R^2
RB	25	5.89×10^{-5}	3.96×10^{-5}	0.1272	0.9346	5.98×10^{-5}	1.04×10^{6}	0.9992
	40	3.25×10^{-5}	74×10^{-1}	−0.0309	0.8377	6.33×10^{-5}	4.96×10^{6}	0.9996
MB	25	1.99×10^{-4}	4.28×10^{-5}	0.0315	0.9588	2.01×10^{-4}	1.86×10^{5}	0.9999
	40	1.65×10^{-4}	1.19×10^{-5}	0.0109	0.7926	1.65×10^{-4}	2.26×10^{5}	0.9999

rate for MB molecules mainly adsorbed inside the pores will be slower [12]. Increasing of temperature from 25 to 40 °C will help for releasing process. Therefore, in binary adsorption system at 40 °C, RB adsorption decreases after 100 min.

Using Eqs. (4)–(6), thermodynamic parameters (ΔG°, ΔH° and ΔS°) for adsorption of MB and RB in binary component system were calculated (Table 5). As can be seen, similar to single component systems, the adsorption is exothermic.

3.2.2. Adsorption kinetics in binary component system

Plot of pseudo-second-order kinetic model for adsorption of MB at 25 and 40 °C in binary component system has been demonstrated in Fig. 8. Results for the competitive adsorption are compared in Table 5. It is clear that pseudo-second-order kinetic model show much better correlation coefficients, close to ideal value in all cases. Thus, similar to single component systems, adsorption of the basic dyes on the adsorbent follows the pseudo-second-order kinetics. As discussed in Section 3.2.1, RB molecules mainly adsorb on surface of the adsorbent. However, adsorption of MB mainly occurs on pores of the adsorbent. For these reasons, it is clear that pseudo-second-order rate constant for adsorption of RB will be greater than that of MB [12].

3.2.3. Effect of solution pH on binary component system

Fig. 9 shows the dynamic adsorption of MB and RB with initial concentration of 8×10^{-5} M onto AlMCM-41 at three different pH and 25 °C in binary component system. It is clear that, similar to single component system, the amount of adsorption capacity of MB and RB increases as the pH increases and then decreases. When pH of solution is changed from 2 to 7, the adsorption will change from 3.33×10^{-5} to 1.96×10^{-4} mol/g and from 1.40×10^{-6} to 3.0×10^{-5} mol/g for MB and RB, respectively. Also, for RB, there is not significant adsorption at pH 12. Moreover, it is clear that adsorption of RB on AlMCM-41 initially increases and then decreases after

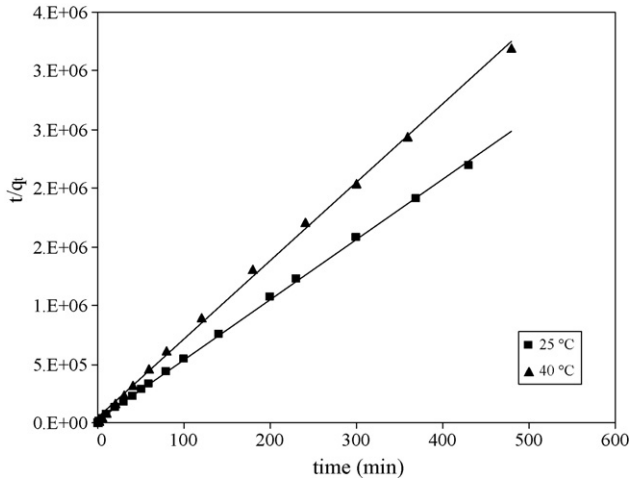

Fig. 8. Pseudo-second-order kinetics for adsorption of MB onto AlMCM-41 in binary component system at 25 and 40 °C.

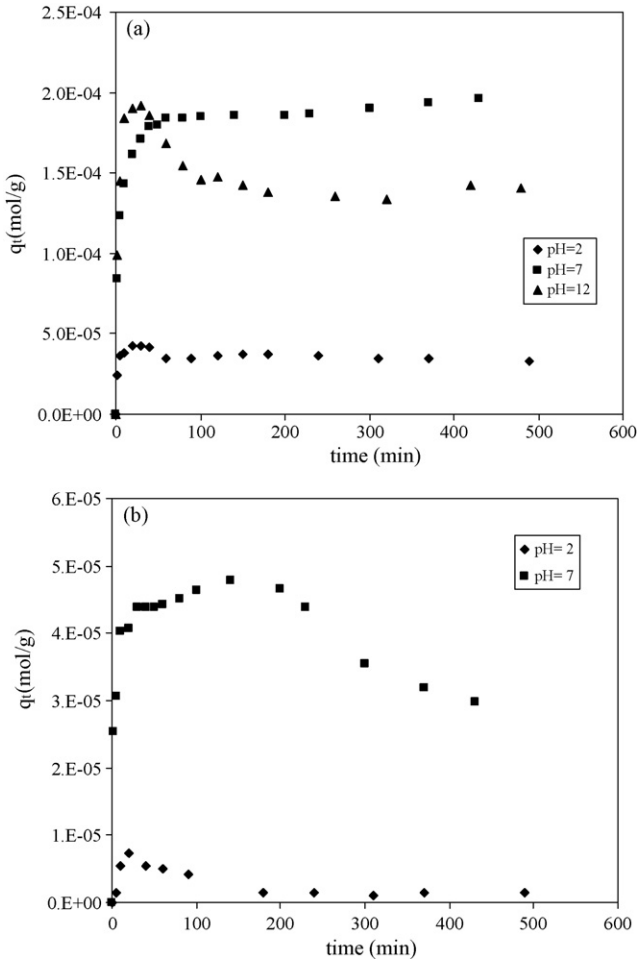

Fig. 9. Dynamic adsorption of MB and RB onto AlMCM-41 in binary component system in various pH at 25 °C (a) MB and (b) RB.

maxima. This can be attributed to the surface adsorption of RB leading to easily releasing by hydrolysis [12]. The decrease of MB adsorption on the adsorbent is mainly occurs at alkaline solution. In alkaline solutions, hydrolysis of some adsorbed MB molecules on surface of the adsorbent by OH^- attach will release MB molecules from the adsorbent. It is clear that, in neutral solutions, hydrolysis rate by water molecules for releasing MB molecules is negligible.

4. Summary

The AlMCM-41 was applied for single and binary component adsorption systems of two basic dyes, MB and RB. It was found that the adsorbent exhibits higher adsorption capacity for MB than RB due to the difference in molecular size. The maximal adsorption capacities for MB and RB are 2.08×10^{-4} and 8.74×10^{-5} mol/g at 25 °C, respectively. For single and binary component systems, the adsorption data were fairly fitted by the Langmuir model. In binary

component system at 25 °C, adsorption of MB and RB is approximately reduced by 94 and 79% of single component adsorption systems, respectively. Kinetics of the adsorption is better described by the pseudo-second-order model. In single and binary component systems, the adsorption extent of MB and RB onto AlMCM-41 increases with pH of solution and then decreases.

References

[1] T. Robinson, G. McMullan, R. Marchant, P. Nigam, Remediation of dyes in textile effluent: a critical review on current treatment technologies with a proposed alternative, Bioresour. Technol. 77 (2001) 247–255.
[2] G. Crini, Non-conventional low-cost adsorbents for dye removal: a review, Bioresour. Technol. 97 (2006) 1061–1085.
[3] N.D. Lourenco, J.M. Novais, H.M. Pinheiro, Effect of some operational parameters on textile dye biodegradation in a sequential batch reactor, J. Biotechnol. 89 (2001) 163–174.
[4] P.P. Selvam, S. Preethi, P. Basakaralingam, N. Thinakaran, A. Sivasamy, S. Sivanesan, Removal of rhodamine B from aqueous solution by adsorption onto sodium montmorillonite, J. Hazard. Mater. 155 (2008) 39–44.
[5] A.K. Jain, V.K. Gupta, A. Bhatnagar, Utilization of industrial waste products as adsorbents for the removal of dyes, J. Hazard. Mater. 101 (2003) 31–42.
[6] V.K. Gupta, A. Mittal, L. Krishnan, V. Gajbe, Adsorption kinetics and column operations for the removal and recovery of malachite green from wastewater using bottom ash, Sep. Purif. Technol. 40 (2004) 87–96.
[7] V.K. Gupta, A. Mittal, L. Krishnan, J. Mittal, Adsorption treatment and recovery of the hazardous dye, Brilliant Blue FCF, over bottom ash and de-oiled soya, J. Colloid Interface Sci. 293 (2006) 16–26.
[8] X.S. Zhao, G.Q. Lu, G.J. Millar, Advances in mesoporous sieve MCM-41, Ind. Eng. Chem. Res. 35 (1996) 2075–2090.
[9] P. Selvam, S.K. Bhatia, C.G. Sonwane, Recent advances in processing and characterization of periodic mesoporous MCM-41 silicate molecular sieves, Ind. Eng. Chem. Res. 40 (2001) 3237–3261.
[10] L.C. Juang, C.C. Wang, C.K. Lee, Adsorption of basic dyes onto MCM-41, Chemosphere 64 (2006) 1920–1928.
[11] K.F. Lam, K.L. Yeung, G. McKay, A rational approach in the design of selective mesoporous adsorbents, Langmuir 22 (2006) 9632–9641.
[12] S. Wang, H. Li, Structure directed reversible adsorption of organic dye on mesoporous silica in aqueous solution, Microporous Mesoporous Mater. 97 (2006) 21–26.
[13] K.F. Lam, K.L. Yeung, G. McKay, Preparation of selective mesoporous adsorbents for $Cr_2O_7^{-2}$ and Cu^{+2} separation, Microporous Mesoporous Mater. 100 (2007) 191–201.
[14] S. Wang, L. Tian, Reversible and irreversible adsorption of dye on mesoporous materials in aqueous solution, Stud. Surf. Sci. Catal. 165 (2007) 227–230.
[15] K.F. Lam, K.L. Yeung, G. McKay, A new approach for Cd^{+2} and Ni^{+2} removal and recovery using mesoporous adsorbent with tunable selectivity, Environ. Sci. Technol. 41 (2007) 3329–3334.
[16] K.F. Lam, C.M. Fong, K.L. Yeung, Separation of precious metals using selective mesoporous adsorbents, Gold Bull. 40 (2007) 192–198.
[17] K.F. Lam, X.Q. Chen, G. McKay, K.L. Yeung, Anion effect on Cu^{+2} adsorption on [$_2$NH]-MCM-41, Ind. Eng. Chem. Res. 47 (2008) 9376–9383.
[18] K.F. Lam, C.M. Fong, K.L. Yeung, G. McKay, Selective adsorption of gold from complex mixtures using mesoporous adsorbents, Chem. Eng. J. 145 (2008) 185–195.
[19] K.F. Lam, X.Q. Chen, C.M. Fong, K.L. Yeung, Selective mesoporous adsorbents for Ag^{+}/Cu^{+2} separation, Chem. Commun. (2008) 2034–2036.
[20] X.Q. Chen, K.F. Lam, Q.J. Zhang, B.C. Pan, M. Arruebo, K.L. Yeung, Synthesis of highly selective magnetic mesoporous adsorbent, J. Phys. Chem. C 113 (2009) 9804–9813.
[21] D. Wei, H. Wang, X. Feng, W. Chuch, P. Ravikovitch, M. Lyubovsky, C. Li, T. Tekeguchi, G.L. Holler, Synthesis and characterization of vanadium-substituted mesoporous molecular sieves, J. Phys. Chem. B 103 (1999) 2113–2121.
[22] M.A. Zanjanchi, Sh. Asgari, Incorporation of aluminum into the framework of mesoporous MCM-41: the contribution of diffuse reflectance spectroscopy, Solid State Ionics 171 (2004) 277–282.
[23] M.A. Zanjanchi, A. Ebrahimian, Z. Alimohammadi, A spectroscopic study on the adsorption of cationic dyes into mesoporous AlMCM-41 materials, Opt. Mater. 29 (2007) 794–800.
[24] Sh. Sohrabnezhad, A. Pourahmad, E. Radaee, Photocatalytic degradation of basic blue 9 by CoS nanoparticles supported on AlMCM-41 material as a catalyst, J. Hazard. Mater. 170 (2009) 184–190.
[25] V. Meshko, L. Markovska, M. Mincheva, A.E. Rodrigues, Adsorption of basic dyes on granular activated carbon and natural zeolite, Water Res. 35 (2001) 3357–3366.
[26] S. Wang, H. Li, L. Xu, Application of zeolite MCM-22 for basic dye removal from wastewater, J. Colloid Interface Sci. 295 (2006) 71–78.
[27] V. Vadivelan, K.V. Kumar, Equilibrium, kinetics, mechanism, and process design for the sorption of methylene blue onto rice husk, J. Colloid Interface Sci. 286 (2005) 90–100.
[28] S. Wang, Z.H. Zhu, Characterisation and environmental application of an Australian natural zeolite for basic dye removal from aqueous solution, J. Hazard. Mater. 136 (2006) 946–952.
[29] J. Yener, T. Kopac, G. Dogu, T. Dogu, Adsorption of Basic Yellow 28 from aqueous solutions with clinoptilolite and amberlite, J. Colloid Interface Sci. 294 (2006) 255–264.
[30] S.K. Alpat, O. Ozbayrak, S. Alpat, H. Akcay, The adsorption kinetics and removal of cationic dye, Toluidine Blue O, from aqueous solution with Turkish zeolite, J. Hazard. Mater. 151 (2008) 213–220.
[31] Q. Cai, Zh-Sh. Luo, W.Q. Pang, Yu-W. Fan, Xi-H. Chen, Fu-Zh. Cui, Dilute solution routes to various controllable morphologies of MCM-41 silica with a basic medium, Chem. Mater. 13 (2001) 258–263.
[32] S. Wang, H. Li, S. Xie, S. Liu, L. Xu, Physical and chemical regeneration of zeolitic adsorbents for dye removal in wastewater treatment, Chemosphere 65 (2006) 82–87.
[33] M.A. Rauf, S.M. Qadri, S. Ashraf, K.M. Al-Mansoori, Adsorption studies of Toluidine Blue from aqueous solutions onto gypsum, Chem. Eng. J. 150 (2009) 90–95.